



Published in final edited form as:

Nanoscale. 2013 April 7; 5(7): 2664–2668. doi:10.1039/c3nr00015j.

'Marker-of-self' functionalization of nanoscale particles through a top-down cellular membrane coating approach

Che-Ming J. Hu^{a,b}, Ronnie H. Fang^{a,b}, Brian T. Luk^{b,c}, Kevin N.H. Chen^a, Cody Carpenter^a, Weiwei Gao^{a,b}, Kang Zhang^{a,d,e}, and Liangfang Zhang^{a,b}

Liangfang Zhang: zhang@ucsd.edu

^aDepartment of NanoEngineering, University of California, San Diego, 9500 Gilman Drive, La Jolla, CA 92093, USA. Tel: 1-858-246-0999

^bMoore's Cancer Center, University of California, San Diego, 9500 Gilman Drive, La Jolla, CA 92093, USA. Tel: 1-858-246-0999

^cDepartment of Bioengineering, University of California, San Diego, 9500 Gilman Drive, La Jolla, CA 92093, USA. Tel: 1-858-246-0999

^dDepartment of Ophthalmology and Shiley Eye Center, University of California, San Diego, 9500 Gilman Drive, La Jolla, CA 92093, USA. Tel: 1-858-246-0999

^eState Key Laboratory of Ophthalmology, Zhongshan Ophthalmic Center, Sun Yat-sen University, Guangzhou 510275, China

Abstract

We investigate the 'marker-of-self' functionalization of nanoparticles through coating of natural RBC membranes. The membrane translocation approach is shown to be highly efficient and bestows nanoparticles with correctly oriented and functional immunomodulatory proteins such as CD47 at equivalent density to natural RBCs.

Enabling active immune evasion through biomimetic surface functionalization presents an emerging stealth strategy for developing long-circulating delivery vehicles.^{1, 2} The identification of CD47, a transmembrane protein that serves as a universal molecular 'marker-of-self', has led to its utilization in the growing development of bio-inspired, immune-evasive devices. Capable of inhibiting phagocytosis and conferring anti-inflammatory properties through interactions with signal regulatory protein alpha (SIRP α) expressed by macrophages, CD47 and its analogs have been found to contribute to the *in vivo* survival of red blood cells (RBCs),³ cancer cells,⁴ and viruses⁵. Application of CD47 to modulate the immune responses against synthetic devices was first demonstrated with macrophages treated by purified recombinant, soluble CD47, which showed reduced uptake of colloidal emulsions.⁶ Synthetic materials covalently conjugated with recombinant CD47 further advanced this biomimetic stealth approach, yielding polymeric microspheres⁷ and implant surfaces with reduced affinity to inflammatory cells.^{8, 9} On nanoscale particles, however, interfacing with native biological components through chemical conjugation of immunomodulatory proteins to particle surfaces can be difficult to manipulate. In particular, inconsistent protein surface density and randomized ligand orientations are notable issues that can greatly undermine the performance of the resulting nanocarriers.

Correspondence to: Liangfang Zhang, zhang@ucsd.edu.

[†]Electronic Supplementary Information (ESI) available: experimental section, theoretical calculations, and supporting figures. See DOI: 10.1039/b000000x/

Toward engineering nanocarriers that can actively suppress immune attack by macrophages, herein we demonstrate a robust ‘top-down’ approach to functionalizing nanoscale particles with native CD47 by cloaking sub-100 nm nanoparticles with cellular membranes derived directly from natural RBCs (Fig. 1). The uniqueness of this membrane coating approach lies in its ability to functionalize nanoparticles with native immunomodulatory proteins including CD47 at an equivalent density to that on natural RBCs. In this study, we show direct evidence that the ‘marker-of-self’ proteins are transferred to the particle surfaces and present in the right-side-out orientation. A macrophage uptake study confirms the stealth functionality conferred by the immunomodulatory proteins. Since cellular membranes anchor the many molecular tags that define cellular identities, attaching these membranes to nanoparticle surfaces provides unparalleled control over the functionalization of synthetic nanocarriers toward biomimicry.

With five membrane-spanning regions, CD47 is an integral membrane protein firmly embedded in RBC membranes, exhibiting an IgV-like extracellular domain that helps maintain the RBCs’ survival in the circulation.¹⁰ While it was previously shown that RBC membrane coating associated nanoparticles with the majority of the membrane materials,¹¹ it remained to be investigated whether these RBC membrane-coated nanoparticles (RBC-NPs) properly present the CD47 for immunomodulation. Verification of the protein, its density, and its orientation on the RBC-NP surfaces demands a molecular examination of these RBC-mimicking nanocarriers. To investigate the functionalization of native CD47 on RBC-NPs, 70 nm poly(lactic-co-glycolic acid) (PLGA) particles were first extruded with RBC membrane-derived vesicles following a previously described protocol.¹¹ Through scanning electron microscopy (SEM) visualization, a spherical morphology was observed for the resulting RBC-NPs (Fig. 2A), and dynamic light scattering measurements showed a mean particle diameter of 85 ± 2 nm (Supplement Fig. S1). The purified particles were then solubilized in a lithium dodecyl sulphate (LDS) sample loading buffer, following which the protein contents stripped from the nanoparticles were separated by SDS-PAGE. The resulting protein gel was subsequently subjected to western blotting using anti-CD47 antibody as the primary immunostain. The presence of CD47 on the RBC-NPs was confirmed by a distinct, single band at 50 kDa (Fig. 2B), which is the characteristic molecular weight of the CD47 protein self-marker.¹⁰

To further examine the extent of CD47 protein on the particle surfaces, the RBC-NPs prepared with different RBC membrane to polymeric particle ratios were collected and analysed for retained CD47 contents. An ultracentrifugation process was applied to isolate the resulting RBC-NPs from free RBC membranes, following which protein contents on the nanoparticles was processed through SDS-PAGE and examined by western blotting analysis. Fig. 2C shows the relative CD47 retention on the different particle formulations. As the RBC membrane to polymeric particle ratio increased from 25 to 150 μ L of blood per mg of polymer, a corresponding increase in the CD47 intensity was observed. This positive correlation reflects the increasing particle functionalization by the increasing RBC membrane inputs, as more CD47 could be identified in the isolated nanoparticle samples. Saturation in CD47 band intensity was observed upon further raising the RBC membrane to polymer ratio above 150 μ L/mg, which reflected the upper limit of CD47 functionalization achievable by the RBC membrane coating. To quantitatively analyze the protein density on the RBC-NPs, CD47 standards were prepared from predetermined volumes of blood, from which CD47 content was estimated based on the average CD47 number on a mouse RBC (16,500 copies per cell)¹² and the RBC concentration in mouse blood (10^{10} cells per mL of blood)¹³ (Supplement discussion and Fig. S2). Comparing the CD47 retention from the different RBC-NP formulations to the protein standards showed that the saturation level corresponded to approximately 2×10^{13} copies of CD47 per mg of polymeric particles (Fig. 2D), yielding on average ~ 5 copies of CD47 per RBC-NP (Supplement discussion). To put

the CD47 density into perspective, the surface area of the 85 nm RBC-NPs was calculated ($\sim 1 \times 10^{11} \mu\text{m}^2/\text{mg}$, Supplement discussion), from which a surface density of ~ 200 molecules of CD47 per μm^2 at saturation on the RBC-NPs can be derived. Given that natural RBCs possess 200–250 copies of CD47 per μm^2 ,^{12, 14} the close match in the CD47 density on the RBC-NPs suggests that the membrane coating brought nearly all of RBCs' CD47 content onto the sub-100 nm particles. The result reflects the robustness of the membrane functionalization technique, as most of the membrane proteins were retained within the cellular membranes throughout the particle preparation process.

It should also be noted that the RBC membrane to polymer ratio corresponding to the onset of CD47 saturation was in close match to the theoretical ratio for complete unilamellar particle coating. Based on surface area estimations, approximately 125 μL of blood is required to completely cover the surfaces of 1 mg of the 70 nm PLGA particles (Supplement discussion). Experimental observations showed that above the ratio of $\sim 130 \mu\text{L}$ of blood/mg PLGA polymer, additional RBC membrane materials did not further functionalize the particles with CD47. As additional membrane materials in excess of complete unilamellar particle coverage were removed during the isolation of RBC-NPs, it can be inferred that the RBC membrane coating precluded further membrane interactions and that multilamellar membrane coating on the nanoparticles was unfavorable. To further investigate the RBC-NP formation under excessive RBC membrane to polymer ratios, RBC-NPs prepared with 250 μL of blood per mg of polymer were visualized under TEM (Supplement Fig. S3). It was found that despite the availability of excess membrane materials in the samples, the nanoparticles were covered by a single, unilamellar coating of lipid membranes with a thickness of 6–8 nm, which is in agreement with the characteristic membrane thickness of RBCs.¹⁵ Excess membranes remained in vesicular forms, which helped to explain the CD47 saturation on the RBC-NPs. In contrast to the unfavored multilamellar coating, unilamellar membrane coating on the RBC-NPs appeared to be highly efficient. By converting the RBC membrane input in Fig. 2D to its corresponding CD47 content (Supplement Fig. S4), the resulting correlation showed that, below the CD47 saturation, approximately 92% of the input membrane proteins were utilized for particle functionalization. This observation suggests that the RBC membrane coating to the PLGA particle surfaces was a favorable process that readily took place. The high efficiency in translocating CD47 onto nanoparticle surfaces confers a unique advantage to the RBC membrane coating approach.

To verify that the CD47 functionalized RBC-NPs possessed the properly oriented self-markers for molecular interactions, the particle surfaces were examined for the presence of CD47's extracellular domains. Rat anti-CD47 antibodies specific to the CD47's extracellular region were applied to the RBC-NPs on a glow-discharged carbon-coated grid. Following 1 min of incubation, the sample was washed and subsequently incubated with anti-rat IgG gold conjugate, which labelled the anti-CD47 antibodies that were retained on the grid. The immunogold-labelled sample was then rinsed with water prior to visualization by transmission electron microscopy (TEM). Fig. 3A shows the attachment of the electron-dense gold particles to multiple gray circular patterns 60–80 nm in diameter, which confirmed that the gold conjugates were attached to the RBC-NPs. A negative control prepared in the absence of the primary stain showed that the gold labelling was specific to the anti-CD47 antibodies (Supplement Fig. S5). Together, these TEM results confirm the presence of right-side-out CD47 on the RBC-NPs. To further examine the presence of inside-out CD47 on the RBC-NPs, a rabbit anti-CD47 antibody that specifically targets an intracellular sequence of CD47 was used. Curiously, while the antibody bound to the CD47 on RBC-NPs in western blotting, it did not yield observable immunogold staining on either RBC-NPs or bare PLGA nanoparticles under TEM (Supplement Fig. S6). These results indicate the relative absence of intracellular CD47 sequences on the particle surfaces. Although the immunostaining experiment provides a qualitative rather than a quantitative

measure of the membrane sidedness on the RBC-NPs, it suggests that the right-side-out membrane orientation was dominant on the RBC-NPs. Given that the extracellular side of RBC membranes possesses a strong negative charge owing to high abundance of sialated moieties¹⁶, it is likely that electrostatic effects favored the interactions between negatively charged polymeric cores and the less negatively charged intracellular side of the RBC membranes, giving rise to a right-side-out orientation bias. This orientation bias also helps explain the unilamellar coating on the RBC-NPs, which could result from the rich surface glycan content that precludes membrane-membrane interactions. Fig. 3B provides a juxtaposition of magnified images of RBC-NPs and the corresponding bare PLGA nanoparticles under negative staining or immunostaining. It can be observed that, following the RBC membrane coating, the particles were bestowed with a unilamellar membrane shell containing CD47 that predominantly exposes their extracellular domains. The proper CD47 orientation is crucial for their molecular interactions.

Lastly, the immunomodulatory effect of the CD47 functionalized RBC-NPs was studied. Bare PLGA nanoparticles and RBC-NPs loaded with hydrophobic DiD fluorophores (excitation/ emission = 644 nm/655 nm) were first incubated with J774 murine macrophage cells and examined for particle internalization. Following 10 min of incubation, the macrophage cells were washed and examined using flow cytometry, which revealed that the RBC membrane coating rendered the particles less prone to the macrophage uptake, resulting in a 64% reduction in particle internalization (Fig. 4). The reduced susceptibility to macrophage engulfment confirmed the translocation of immune-evasive functionality from RBCs to RBC-NPs and helped to explain the long *in vivo* circulation previously observed for the RBC-NPs.¹¹ To identify CD47's contribution to RBC-NPs' immune-evasive property, saturating amounts of anti-CD47 antibodies were applied to the RBC-NPs to block the right-side-out CD47 proteins. The antibody blocking was previously demonstrated to disrupt SIRP α signalling and increased macrophage engulfment of RBCs.¹⁷ Similarly, depriving the particles of the molecular protection from phagocytosis resulted in an increase in particle internalization by 20%, which confirmed the immunomodulatory functionality conferred by the particle-bound CD47. Curiously, the CD47-blocked RBC-NPs remained significantly more "stealthy" than the bare PLGA nanoparticles. Given that RBCs have a variety of proteins and glycans on their surface, many of which have been identified to modulate their immunological properties,^{18, 19} other surface moieties in addition to CD47 on the RBC-NPs likely functioned collectively to inhibit the macrophage activity. Future studies are warranted to verify these other membrane moieties and to examine their implications in nanodevice functionalization.

Conclusions

In summary, RBC membrane coating was demonstrated to functionalize sub-100 nm substrates with native CD47, yielding nanoparticles with equivalent CD47 surface density to natural RBCs. Right-side-out CD47 proteins were identified on the particle surfaces, readily exposing their extracellular domain for molecular interactions. The immune-evasive property of the RBC-NPs, as indicated by their reduced susceptibility to macrophage uptake, further verified the presence of functional immunomodulatory proteins on the particle surfaces. These biomimetic nanocarriers have tremendous potential in drug delivery applications, as they provide the opportunity to actively inhibit the immune clearance of their therapeutic cargo, thereby improving drug pharmacokinetics and therapeutic efficacy. The in-depth examination of the RBC-NPs also provides an up-close look at the fusion process between RBC membranes and PLGA polymeric particles, which appears to favour the formation of unilamellar membrane coated particles with the right-side-out membrane orientation. From synthesis and fabrication perspectives, the membrane coating technique contrasts with bottom-up functionalization schemes, which often employ chemical

conjugation methods that can alter proteins' innate structures. The non-disruptive protein functionalization through the coating of natural cellular membranes presents a robust and versatile approach in interfacing synthetic materials with biological components, offering a compelling technique for the development of bio-inspired and biomimetic nanodevices.

Supplementary Material

Refer to Web version on PubMed Central for supplementary material.

Acknowledgments

This work is supported by the National Science Foundation Grant DMR-1216461. R.F. is supported by the Department of Defense (DoD) through the National Defense Science & Engineering Graduate Fellowship (NDSEG) Program. B.L. is supported by a National Institutes of Health R25CA153915 training grant from the National Cancer Institute.

Notes and references

1. Yoo JW, Irvine DJ, Discher DE, Mitragotri S. *Nat Rev Drug Discov.* 2011; 10:521–535. [PubMed: 21720407]
2. Balmert SC, Little SR. *Adv Mater.* 2012; 24:3757–3778. [PubMed: 22528985]
3. Oldenburg PA, Zheleznyak A, Fang YF, Lagenaur CF, Gresham HD, Lindberg FP. *Science.* 2000; 288:2051–2054. [PubMed: 10856220]
4. Jaiswal S, Jamieson CH, Pang WW, Park CY, Chao MP, Majeti R, Traver D, van Rooijen N, Weissman IL. *Cell.* 2009; 138:271–285. [PubMed: 19632178]
5. Cameron CM, Barrett JW, Mann M, Lucas A, McFadden G. *Virology.* 2005; 337:55–67. [PubMed: 15914220]
6. Hsu YC, Acuna M, Tahara SM, Peng CA. *Pharm Res.* 2003; 20:1539–1542. [PubMed: 14620504]
7. Tsai RK, Rodriguez PL, Discher DE. *Blood Cells Mol Dis.* 2010; 45:67–74. [PubMed: 20299253]
8. Finley MJ, Rauova L, Alferiev IS, Weisel JW, Levy RJ, Stachelek SJ. *Biomaterials.* 2012; 33:5803–5811. [PubMed: 22613135]
9. Stachelek SJ, Finley MJ, Alferiev IS, Wang F, Tsai RK, Eckells EC, Tomczyk N, Connolly JM, Discher DE, Eckmann DM, Levy RJ. *Biomaterials.* 2011; 32:4317–4326. [PubMed: 21429575]
10. Brown EJ, Frazier WA. *Trends Cell Biol.* 2001; 11:130–135. [PubMed: 11306274]
11. Hu CM, Zhang L, Aryal S, Cheung C, Fang RH, Zhang L. *Proc Natl Acad Sci U S A.* 2011; 108:10980–10985. [PubMed: 21690347]
12. Subramanian S, Tsai R, Sen S, Dahl KN, Discher DE. *Blood Cells Mol Dis.* 2006; 36:364–372. [PubMed: 16697668]
13. Russell ES, Neufeld EF, Higgins CT. *Proc Soc Exp Biol Med.* 1951; 78:761–766. [PubMed: 14912022]
14. Mouro-Chanteloup I, Delaunay J, Gane P, Nicolas V, Johansen M, Brown EJ, Peters LL, Van Kim CL, Cartron JP, Colin Y. *Blood.* 2003; 101:338–344. [PubMed: 12393467]
15. Hochmuth RM, Evans CA, Wiles HC, McCown JT. *Science.* 1983; 220:101–102. [PubMed: 6828875]
16. Jan KM, Chien S. *J Gen Physiol.* 1973; 61:638–654. [PubMed: 4705641]
17. Oldenburg PA, Gresham HD, Lindberg FP. *J Exp Med.* 2001; 193:855–862. [PubMed: 11283158]
18. Hu CM, Fang RH, Zhang L. *Adv Healthcare Mater.* 2012; 1:537–547.
19. Durocher JR, Payne RC, Conrad ME. *Blood.* 1975; 45:11–20. [PubMed: 803103]

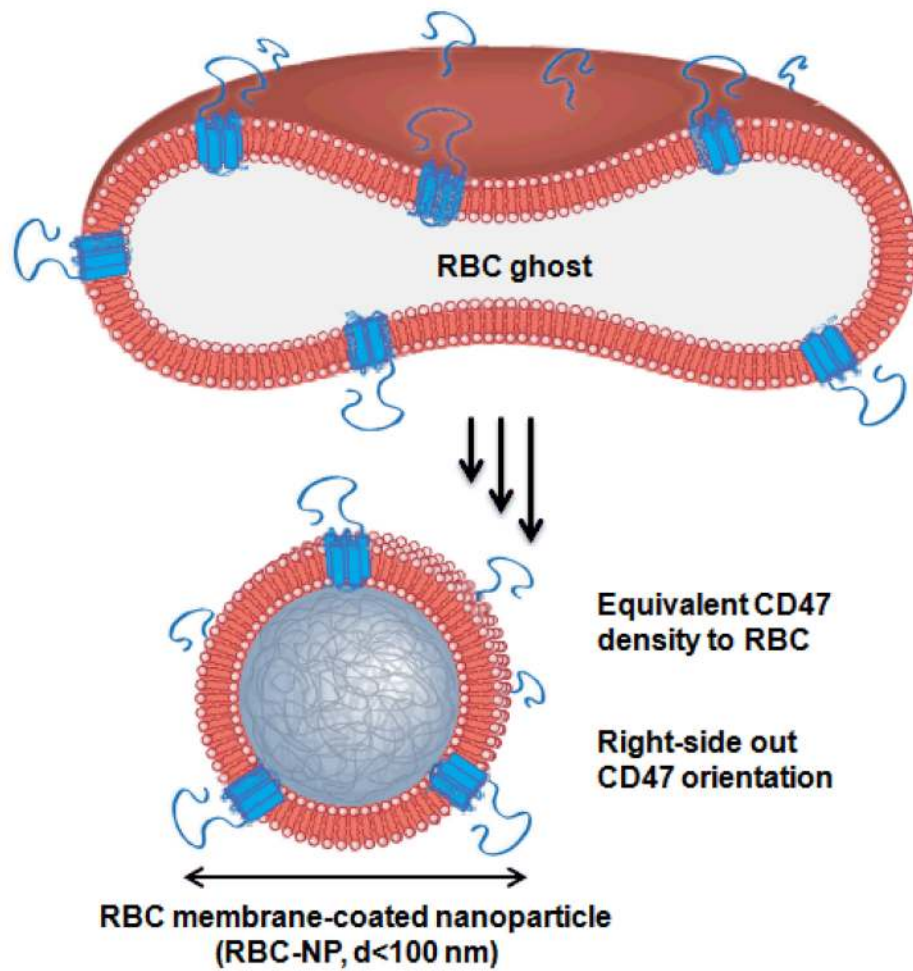


Fig. 1. Schematic of controlled CD47 functionalization on nanoparticles enabled by RBC membrane coating. The resulting RBC membrane-coated nanoparticle (RBC-NP) is expected to have a CD47 density equivalent to that on a natural RBC.

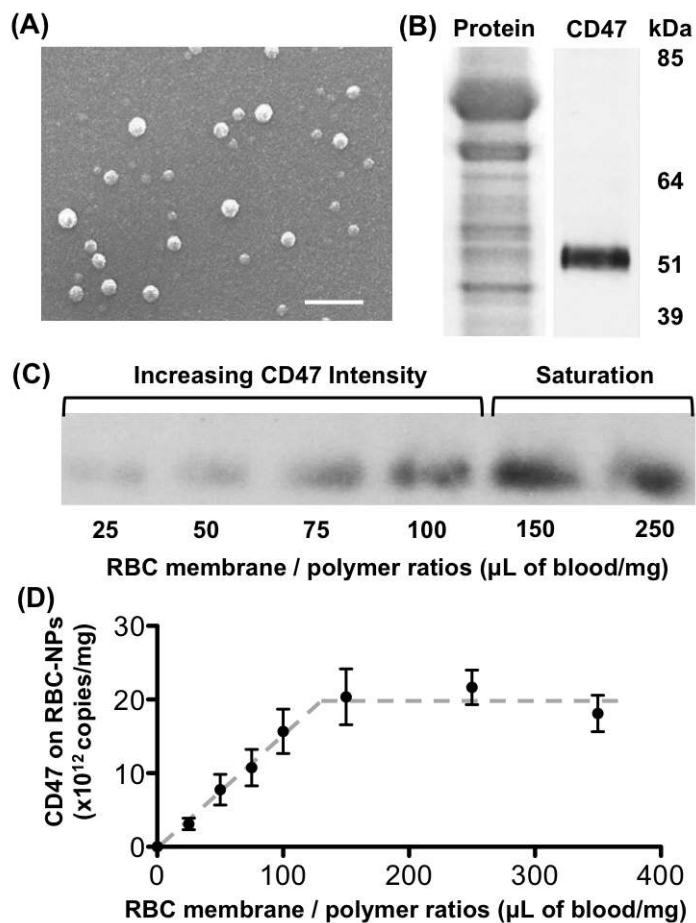


Fig. 2. Characterization and quantification of CD47 on the RBC-NPs. (A) A representative scanning electron microscopy (SEM) image shows the spherical structure and morphology of the prepared RBC-NPs (scale bar = 250 nm). (B) Coomassie staining (left) and CD47 western blot (right) of the RBC-NPs' protein contents following SDS-PAGE separation. (C) Comparison of CD47 contents on the RBC-NPs prepared from different RBC membrane to polymer ratios. (D) Quantitative analysis of CD47 density on the RBC-NPs prepared from different RBC membrane to polymer ratios (n=5).

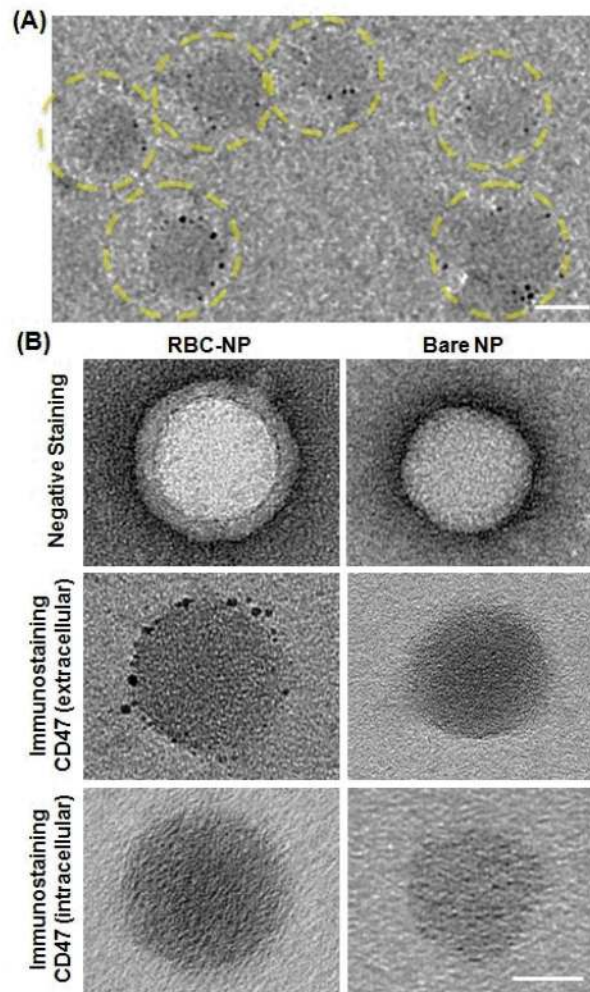


Fig. 3. CD47 orientation on the RBC-NPs. (A) A representative transmission electron microscopy (TEM) image of the RBC-NPs under immunostaining, consisting of a primary stain by rat anti-mouse CD47(extracellular) antibodies and a secondary stain by anti-rat IgG gold conjugates (scale bar = 50 nm). (B) Comparison of the RBC-NPs immunostained with anti-CD47 antibodies that target either the extracellular or the intracellular protein domains and the corresponding bare PLGA nanoparticles (bare NPs) under negative staining with uranyl acetate (scale bar = 30 nm).

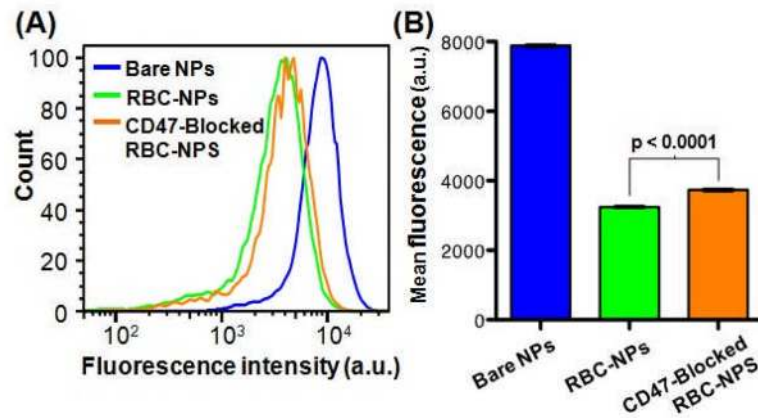


Fig. 4. Inhibition of macrophage uptake. (A) Flow cytometry analysis of particle internalization by murine macrophage cells. The blue, green, and orange lines represent the bare PLGA nanoparticles (bare NPs), RBC-NPs, and CD47-blocked RBC-NPs, respectively. (B) Mean fluorescence intensity reflecting the overall particle uptake by the macrophage cells.